FORUM

Population-level mechanisms for reddened spectra in ecological time series

H. RESIT AKÇAKAYA, JOHN M. HALLEY* and PABLO INCHAUSTI†

*Applied Biomathematics, 100 North Country Road, Setauket, NY 11733, USA, *Department of Ecology, School of Biology, Aristotle University, U.P. Box 119, 54006, Thessaloniki, Greece, e-mail: jmax@bio.auth.gr, and †Laboratoire d'Ecologie, Ecole Normale Supérieure, 46 rue d'Ulm, Paris 75005 France, e-mail: inchausti@biologie.ens.fr*

Summary

1. The temporal variability of many animal populations increases with the length of census period. This pattern is associated with the reddened spectral colour, quantified by the spectral exponent, which is typically around + 1.
2. We used simulation models to explore the effects of various population-level processes on the spectral colour of the simulated time series of abundances.
3. Our results showed that the observed spectral exponents could be explained as the effect of a combination of measurement error and natural variability (in the form of white environmental noise).
4. Thus, it may not be necessary to invoke complex varieties of environmental noise to explain the observed spectral exponents.

Key-words: spectral colour, measurement error, observation error, density dependence, temporal variability

Journal of Animal Ecology (2003) **72**, 698–702

Introduction

A pervasive feature of the long-term ecological time series is that their temporal variability of population abundance typically increases with the length of the census (Pimm 1991; Inchausti & Halley 2001, 2002). This may have important consequences for the estimation of extinction risk (Lawton 1988), although its expected consequences have been subject to debate (Ripa & Lundberg 1996; Cuddington & Yodzis 1999; Halley & Kunin 1999).

The increasing temporal variability of ecological time series may be associated with 'spectral reddening' (Inchausti & Halley 2002), which occurs when power is concentrated at low frequencies of the power spectrum, indicating an overriding importance for long-term trends in the variability of time series data. This may be quantified by the spectral exponent, ν, estimated by the magnitude of the *downward* regression slope on a log-log scale. For reddened processes, ν is positive, in a white noise process it is around zero, while for 'blue noise' process it is negative.

Correspondence: H. Resit Akçakaya, Applied Biomathematics, 100 North Country Road, Setauket, NY 11733, USA. Tel.: +1 631 751 4350. Fax: 1 631 751 3435. E-mail: resit@ramas.com.

Ecologically, temporal variability may be thought of in terms of two contrasting processes: white noise and random walk. White noise describes a completely uncorrelated random process fluctuating within a well-defined range of values and has a spectral exponent of zero, indicating that events at all frequencies approximately explain similar amount of the variability of the time series. By contrast, a population executing a random walk progressively accumulates random, uncorrelated increments of population abundance over time, leading to a linear increase of population variability with the length of the data series (Halley & Kunin 1999) and an expected spectral exponent of +2. Long-term (> 30 years) time series of animal populations censused annually typically have reddened dynamics with an overall mean value of +1·02 (SE = 0·04) (Inchausti & Halley 2001, 2002), which is 'halfway' between white noise and the random walk, sharing some properties of each. Population dynamics may become 'reddened' in several ways, by inherited redness from variation in the environment (Lawton 1988), through species interactions (Miramontes & Rohani 1998; Ripa, Lundberg & Kaitala 1998), stochastic delayed density dependence (Kaitala & Ranta 1996), spatially explicit (White, Begon & Bowers 1996) or age-structured (MacArdle 1989) dynamics. However, in an experimental study of single isolated populations, Petchey (2000) found that

all populations had reddened spectra regardless of the colour of the environmental fluctuations, and concluded that it may not be necessary to explain reddened dynamics with extrinsic influences.

In this paper, we examine the effect of various general population-level processes on the spectral colour of the resulting time series. In other words, we explore some within-population mechanisms that generate reddened spectra similar to the ones found for wild animal populations. We assume that the environmental fluctuations are white noise at the annual time scale of population dynamics (e.g. Lovejoy & Schertzer 1986; Swanson 1998). Spectral analysis of historical meteorological data (Pelletier 1997) shows that while environmental variability is strongly reddened on short time scales (ν = 1·37, for days to months), the reddening is much weaker over timescales of interest (ν = 0·37, for seasons to hundreds of years) when examining the dynamics of ecological populations. We considered combinations of environmental variation, demographic stochasticity, intensity of density dependence and age structure to examine the relative importance of these factors in producing the type of reddened variation observed in natural populations. Because natural populations are rarely subject to complete censuses, it is essential to consider the influence of measurement error if we are to compare the degree of spectral reddening generated by the models with the values estimated from long-term time series of wild populations.

Methods

MODEL COMPONENTS

Our approach consisted of generating sets of time series with a discrete-time, single-population model, and then analysing each time series to calculate its spectral exponent. We generated time series of length 64 time steps (years), because longer time series of natural populations are actually very rare (Inchausti & Halley 2002). Using RAMAS Metapop (Akçakaya 2002), we created single-population models with and without age structure, with and without demographic stochasticity, and various levels of density dependence, natural variability and observation error. These model components are described below, followed by an example.

Age structure. Scalar models (without age structure) had an average population growth rate, $R = 1·0$. For models with age structure, we used the following Leslie matrix with three age classes:

$$\begin{pmatrix} n_0' \\ n_1' \\ n_2' \end{pmatrix} = \begin{bmatrix} 0 & 0 & 0·4 \\ 0·625 & 0 & 0 \\ 0 & 0·8 & 0·8 \end{bmatrix} \begin{pmatrix} n_0 \\ n_1 \\ n_2 \end{pmatrix} \qquad \text{eqn 1}$$

This model leads to a stationary population ($\lambda = 1·0$) and a generation time of about seven time steps (years). The number of individuals (N) was defined as the total of individuals in all age classes. All models were started from the stable age distribution.

Density dependence. Several levels of density dependence (from none or exponential growth to strong) were modelled with a Ricker equation. For the scalar model $N(t + 1) = R(t) \cdot N(t)$, the growth rate at time step t, $R(t)$, was set as

$$R(t) = R_{\max} \cdot \exp\left(\frac{-\ln(R_{\max}) \cdot N(t)}{K} \right) \qquad \text{eqn 2}$$

where $R_{\max}$ is the maximum rate of growth, K is the carrying capacity, and $N(t)$ is the number of individuals at time t. The number at the start of the simulation, $N(0)$, was always set to 0·625K. Weak and strong density dependence were modelled with $R_{\max} = 1·1$ and 2·0, respectively. In addition, moderate levels with $R_{\max} = 1·3$ and 1·6 were modelled. When age structure (see above) was used, all elements of the Leslie matrix were changed proportionally at each time step to make the eigenvalue of the matrix equal to the growth rate in equation 2 (for details, see Akçakaya 2002).

Demographic stochasticity. In models without demographic stochasticity, abundances were rounded to nearest integer and equilibrium was chosen so that and average abundance was between 9000 and 10000. In models with demographic stochasticity, the number of survivors was selected from binomial, and number of offspring from Poisson distributions (Akçakaya 1991); the average abundance was between 900 and 1000.

Variability. Two types of variability were modelled. Temporal variability of the demographic rates was modelled by selecting the population growth rate R (in the case of scalar models), or the mortality and fecundity rates (in the case of age-structured models) from lognormal distributions with a given coefficient of variation, CV_N. Observation (measurement) error was modelled by sampling the observed abundance (N_{obs}) from a normal distribution with the given coefficient of variation for measurement error, CV_E, and with uncorrelated magnitudes over time (i.e. a white noise process).

Example. A scalar, density-independent model with demographic stochasticity, natural variation, and measurement error is:

$$N(t + 1) = \text{Poisson}(R(t) \cdot N(t)) \qquad \text{eqn 3}$$

where $R(t)$ is sampled from a lognormal distribution with mean = 1·0 and coefficient of variation for natural variability, CV_N. Based on this simulated abundance, the 'observed' abundance N_{obs} is calculated using $N_{\text{obs}}(t + 1) = N(t + 1) \cdot (1 + CV_E \cdot r)$, where r is a standard normal deviate (with mean = 0 and variance = 1). Because of the small to moderate magnitude of CV_E, this calculation did not cause zero or negative abundance in any of our simulations.

ANALYSIS

For each combination of model components, we created 100 time series of length 64 and performed a spectral
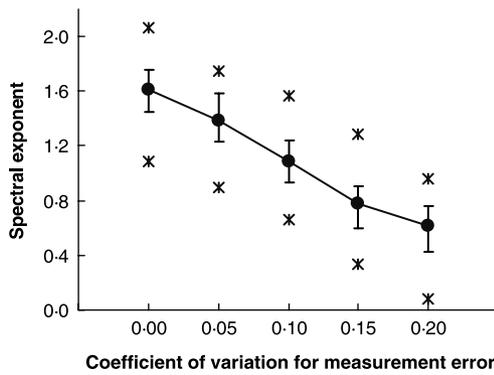
Fig. 1. Spectral exponent as a function of the magnitude of measurement error, in models with no density dependence, no age structure, no demographic stochasticity. Environmental stochasticity was modelled with lognormally distributed growth rates with mean of 1 and CV of 0·1. Median (●), quartiles (error bars), and the 95% confidence interval (×) at each level of measurement error are based on 100 simulated trajectories.
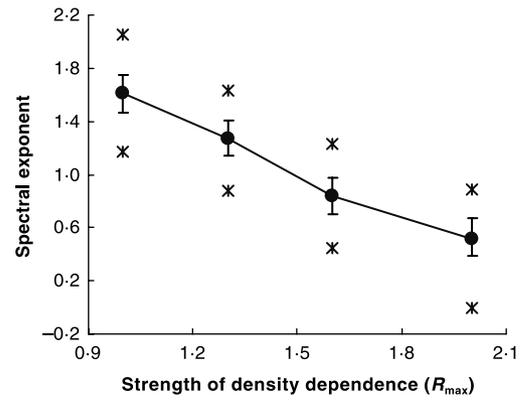
Fig. 2. Spectral exponent as a function of the strength of density dependence, in models with no measurement error, no age structure, no demographic stochasticity. Environmental stochasticity was modelled with lognormally distributed growth rates with mean of 1 and CV of 0·1. Median (●), quartiles (error bars), and the 95% confidence interval (×) at each level of density dependence are based on 100 simulated trajectories.

analysis on each of the log-transformed time series. The outcome of this analysis is spectral power (expressed in units of variance for each frequency) whose magnitude is proportional to the total variance explained by that frequency. The spectral analyses were carried out in STATISTICA using a Hamming window. For each time series, a spectral exponent was estimated as the regression slope of spectral power vs. frequency (on a log-log scale). Thus, for each combination of model components, we estimated 100 spectral exponents and summarized the results in terms of the median, the quartiles, and the 95% confidence interval of these 100 spectral exponent estimates.

Results

An increase in the magnitude of measurement error caused a decrease in spectral exponents (Fig. 1). Except when density dependence was strong (see below), the median spectral exponent ranged from 1·5 to 1·6 when all variation is natural, from −0·1 to 0·6, when all variation is measurement error, and from 1·0 to 1·2 when natural variation and measurement error were comparable (Table 1). In a density-independent model

with CV for environmental stochasticity equal to the CV for measurement error, the median spectral exponent was 1·09 with 95% confidence interval of 0·66–1·57 (Fig. 1).

Increased strength of density dependence caused a decrease in spectral exponents (Fig. 2). When there was no density dependence or when density dependence was weak, the spectral exponent was strongly dependent on how much of the variation was natural vs. measurement error (see above). When density dependence was strong, the median spectral exponent ranged from 0·2 to 0·5; when it was weak the median spectral exponent was around 1·5 (with only natural variation) and 0·5 (with only measurement error) (Table 1). In a model with moderate density dependence ($R_{max} = 1·3$), the median spectral exponent was 1·27 with 95% confidence interval of 0·88–1·64 (Fig. 2).

Age structure and demographic stochasticity did not have a strong effect on the median spectral exponent (Table 1). In contrast, demographic stochasticity caused a slight decrease in the median exponent, especially when all variation was due to measurement error (Table 1).

Table 1. Median spectral exponent for 15 combinations of parameters (each median is based on 100 simulated trajectories)

Model components			Median spectral exponent		
Age structure	Density dependence	Demographic stochasticity	Only natural variation ($V_N = 10\%$)	Both natural variation ($V_N = 5\%$) and measurement error ($V_E = 5\%$)	Only measurement error ($V_E = 10\%$)
No	No	No	+1·63	+1·01	−0·07
No	No	Yes	+1·64	+1·17	+0·38
No	Weak	Yes	+1·47	+1·13	+0·53
Yes	Weak	Yes	+1·50	+1·09	+0·56
No	Strong	Yes	+0·52	+0·46	+0·21

Discussion

The models with no density dependence and no observation error produced, as expected, a random walk whose spectral exponents approached the expected value of 2. The models with observation error (but no natural variability or density dependence) produced time series with spectral exponents around 0. This is not surprising, because in the absence of natural variability, the models were deterministic with a constant N, and the only variation resulted from observation error that was modelled as a white noise process. When both measurement error and natural variability are present (as is probably the case for the vast majority of observed time series), the spectral exponent is around 1 (the only exception to this is strong density dependence; see below).

Interestingly, when observation error and natural variability have comparable magnitudes, the spectral exponents range from about 0·5–1·5, with a median close to 1·0, as observed in time series of animal populations (Inchausti & Halley 2001, 2002). The results show that the distribution of spectral exponents of observed time series of animal populations could be explained as the effect of a combination of measurement error and natural variability.

Although it is clear that many, if not all, ecological time series include measurement or observation error, there are few studies in which the relative contributions of observation error and natural variability are estimated, because this requires having independent, replicated estimates of the abundance of the same population at the same time step(s) by different observers or by different methods (Link & Nichols 1994). A recent study estimated that about 50% of the observed variance in the time series of 1-year-old striped bass could be ascribed to measurement error (Dunning *et al.* 2002). In an analysis of observation error in 10 studies involving 20 species, the average absolute deviation from the true population count was 21% (ranging from a 59% underestimate to a 126% overestimate), and two-thirds of observation error estimates fell within 32% of the actual population sizes (Meir & Fagan 2000). However, estimates of natural variation were not provided, presumably because these studies did not involve time series. In an analysis of time series of annual survival rates for several species of sparrows, about 53% of the observed temporal variance was due to sampling error (Sandercock & Jaramillo 2002).

The strength of density dependence produced an effect on the spectral exponents that was similar to that of measurement error. No density dependence (as mentioned above) gave rise to a random walk. When the population modelled was tightly regulated around a carrying capacity, the time series was closer to white noise, regardless of the nature of variation. Weak or moderate density dependence produced time series with spectral exponents ranging from about 0·5–1·5, as observed in time series of animal populations. These results may also be interpreted to mean that most observed time series of abundances contain both natural variation and measurement error, and most populations are not regulated by very strong density dependence (which produces time series with spectral exponents < 0; Cohen 1995).

In summary, it may not be necessary to invoke complex varieties of environmental 'noise' in order to explain the distribution the spectral exponents in the observed time series of animal abundances, whose typical value of +1 spectral exponent may be caused by white environmental noise affecting a population that is observed with measurement error or is subject to weak or moderate density dependence.

References

Akçakaya, H.R. (1991) A method for simulating demographic stochasticity. *Ecological Modelling*, **54**, 133–136.

Akçakaya, H.R. (2002) *RAMAS Metapop: Viability Analysis for Stage-Structured Metapopulations* Version 4·0pr. Applied Biomathematics, Setauket, NY.

Cohen, J. (1995) Unexpected dominance of high frequencies in chaotic nonlinear population models. *Nature*, **378**, 610–612.

Cuddington, K. & Yodzis, P. (1999) Black noise and population persistence. *Proceedings Royal Society London B*, **266**, 969–973.

Dunning, D., Ross, Q., Munch, S. & Ginzburg, L.R. (2002) Measurement error affects risk estimates for recruitment to the Hudson River stock of striped bass. *Thescientificworldjourn*, **2** (S1), 238–253.

Halley, J. & Kunin, W. (1999) Extinction risk and the 1/f family of noise models. *Theoretical Population Biology*, **56**, 215–239.

Inchausti, P. & Halley, J. (2001) Investigating long-term ecological variability using the Global Population Dynamics Database. *Science*, **293**, 655–657.

Inchausti, P. & Halley, J. (2002) The long-term temporal variability and spectral colour of animal populations. *Evolutionary Ecology Research*, **4**, 1033–1048.

Kaitala, V. & Ranta, E. (1996) Red/blue chaotic power spectra. *Nature*, **381**, 198–199.

Lawton, J. (1988) More time means more variation. *Nature*, **334**, 563.

Link, W. & Nichols, J. (1994) On the importance of sampling variance to investigations of temporal variation in animal population. *Oikos*, **69**, 539–544.

Lovejoy, S. & Schertzer, D. (1986) Scale invariance in climatological temperatures and the local spectral plateau. *Annales Geophysicae*, **4B**, 401–410.

MacArdle, B. (1989) Bird population densities. *Nature*, **338**, 628.

Meir, E. & Fagan, W.F. (2000) Will observation error and biases ruin the use of simple extinction models? *Conservation Biology*, **14**, 148–154.

Miramontes, O. & Rohani, P. (1998) Intrinsically generated coloured noise in laboratory insect populations. *Proceedings Royal Society London B*, **265**, 785–792.

Pelletier, J. (1997) Analysis and modeling of the natural variability of climate. *Journal of Climate*, **10**, 1331–1342.

Petchey, O. (2000) Environmental colour affects aspects of single-species population dynamics. *Proceedings Royal Society London B*, **267**, 747–754.

Pimm, S. (1991) *The Balance of Nature? Ecological Issues in the Conservation of Species and Communities*. Chicago University Press, Chicago.

Ripa, J. & Lundberg, P. (1996) Noise colour and the risk of population extinction. *Proceedings Royal Society London B*, **263**, 1751–1753.

Ripa, J., Lundberg, P. & Kaitala, V. (1998) A general theory of

702

H. R. Akçakaya,
J. M. Halley &
P. Inchausti

environmental noise in ecological food webs. *American Naturalist*, **151**, 256–263.

Sandercock, B.K. & Jaramillo, A. (2002) Annual survival rates of wintering sparrows: assessing demographic consequences of migration. *Auk*, **119**, 149–165.

Swanson, B. (1998) Autocorrelated rates of change in animal populations and their relationship to precipitation. *Conservation Biology*, **12**, 801–808.

White, A., Begon, M. & Bowers, R. (1996) Red/blue chaotic power spectra. *Nature*, **381**, 198.